water

MDPI

Article

Distribution Characteristics and Formation Mechanisms of Highly Mineralized Groundwater in the Hetao Plain, Inner Mongolia

Qiuyao Dong [1,2], Jincheng Li [3,†], Yanpei Cheng [1,2,*], Yu Ren [1,2], Dong Zhang [4], Dong Wang [5], Xiaoyue Sun [6] and Wengeng Cao [1,2,†]

1 The Institute of Hydrogeology and Environmental Geology, Chinese Academy of Geosciences, Shijiazhuang 050061, China
2 Hebei Cangzhou Groundwater and Land Subsidence National Observation and Research Station, Shijiazhuang 050061, China
3 Shui Fa Planning and Design Co., Ltd., Jinan 250013, China
4 School of Water Resources and Environment, China University of Geosciences (Beijing), Beijing 100083, China
5 Shandong Harmony Project Consulting Co., Ltd., Jinan 250062, China
6 College of Surveying and Geographic Informatics, North China University of Water Resources and Electric Power, Zhengzhou 450011, China
* Correspondence: ljc970903@163.com
† These authors contributed equally to this work.

Abstract: As the largest artesian irrigation area in northern China, the Hetao Plain is also one of the major grain-producing areas in China. Meanwhile, there is a large amount of highly mineralized groundwater resulting in the soil salinization and desertification in this region. In addition, this study also uses the traditional hydro-geochemical methods to investigate the spatial evolution characteristics and formation mechanisms of highly mineralized groundwater. The results indicate that there is a large amount of highly mineralized groundwater (salinity > 3 g/L) in the shallow aquifer over the Hetao Plain. As far as the spatial patterns are concerned, there are significant spatial differences. In accordance with the structural, paleogeographic, landform, and hydrogeological conditions, the highly mineralized groundwater in the Hetao Plain can be divided into five zones, namely, the front fan depression, the north bank of the Yellow River, Xishanzui, Hasuhai in the Hubao Plain, and Dalad banner on the south bank of the Yellow River. Among them, the highly mineralized groundwater of Xishanzui exhibits the largest value of the salinity > 10 g/L. The main cations are Mg^{2+} and Na^{+}, while the main anions are Cl^{-} and $SO_4{}^{2-}$. Moreover, the groundwater in the highly mineralized area contains a large amount of I^{-}. According to the analysis of Piper, Gibbs diagrams of groundwater, the proportion coefficients of various components and the indication of isotope, it can be seen that most of the chemical ions in groundwater in the highly mineralized zone come from evaporation-concentration, which are mainly affected by climate, sedimentary environment, hydrogeological conditions and hydrology. The source of high mineralization in Xishanzui are different from other high mineralization regions, and the highly mineralized groundwater in Xishanzui is formed by the infestation of deep underground salt brine. These results can provide scientific basis for the rational allocation of regional water resources and the promotion of water resources development and utilization.

Keywords: highly mineralized groundwater; hydrogeochemical methods; distribution characteristics; enrichment mechanism; Hetao Plain

Citation: Dong, Q.; Li, J.; Cheng, Y.; Ren, Y.; Zhang, D.; Wang, D.; Sun, X.; Cao, W. Distribution Characteristics and Formation Mechanisms of Highly Mineralized Groundwater in the Hetao Plain, Inner Mongolia. *Water* **2022**, *14*, 3247. https://doi.org/10.3390/w14203247

Academic Editor: Adriana Bruggeman

Received: 29 August 2022
Accepted: 11 October 2022
Published: 14 October 2022

1. Introduction

Highly mineralized water, also known as mineralized water, refers to water with a salinity greater than 3000 mg/L [1]. The unscientific mining and use of highly mineralized water will cause certain damage to the local ecological environment, such as the increase in

salinity of river water, the raising of shallow groundwater level, the growth of salinization in the soil, the intolerance of saline-alkali weakened forest tree vigor, and reduction in crop production [2,3]. Therefore, it is essential not only to obtain the spatial distribution of highly mineralized groundwater, but also to investigate the formation mechanisms, so as to improve the health and living standards of local residents.

The Hetao Plain of Inner Mongolia is the largest Yellow River irrigation area and also one of the important food production areas over China [4,5]. Due to its unique natural geography, geology, hydrology, and physical chemistry, the groundwater of the Hetao Plain not only contains the arsenic, but also distributes a wide range of highly mineralized water. Especially in the later period of human transformation, the salt content is further accumulated, making the distribution law of highly mineralized groundwater in the area more complicated [6]. Arsenic (As) is one of the most studied elements worldwide due to its harmful impact on the environment and human health. [7] This highly mineralized water seriously affects agricultural productivity, the aquatic environment, and human health. [8]

The research and investigation on the hydrochemical characteristics of groundwater in the Hetao Plain of Inner Mongolia has been carried out for more than 60 years. It can be traced back to the 1950s when the Hetao Plain initiated the "Regional Hydrogeological Survey of 1:200,000". With the gradual deepening of the survey work, hydrogeological surveys of typical problems have been successively launched. However, the specific elements in the groundwater were mainly concentrated on the characteristics of the environment and the impact on the ecology and health of the soil and groundwater in the early stage of the census work [9–11]. In 1982, the study on the hydrogeological conditions and improvement methods of soil salinization in the Hetao Plain was carried out, and the formation and distribution of groundwater in the Hetao Plain, as well as the distribution and dynamics of underground high-mineralized water were ascertained, which opened the prelude to the investigation of highly mineralized groundwater in the Hetao Plain [10,11]. Inner Mongolia completed a 1:500,000 geological environmental survey in 2004, and generally identified the geological environmental problems (e.g., water depletion, ground deformation, deterioration of water quality, and deterioration of the ecological environment) caused by the excessive exploitation of groundwater in this region [12]. Through groundwater resources survey in 1984 and 2000, the evolution process of shallow groundwater was basically ascertained, such as compensation and drainage conditions, dynamic characteristics, and hydro-geochemical characteristics, providing a basic guarantee for water quality improvement and national economic planning [13,14]. With the gradual deepening of the hydrogeological survey, relevant theoretical research is also gradually carried out [15]. In terms of the research on the hydro-chemical evolution of groundwater, Guo, et al. [16] explored the distribution characteristics and genesis of the high concentration arsenic and high fluorine groundwater in the Hetao Plain.

In inland environments, increased groundwater mineralization caused by overexploitation of groundwater has brought many problems for agriculture, drinking water supplies and ecosystems dependent on groundwater [17–19]. Aquifers are layered systems in which the hydrogeological path of waters extends from highly weathered, shallow, and porous rocks to poorly weathered, deep and fissured rocks. This varying hydrogeological setting influences the water chemistry in different ways [20]. Kohfahl, et al. [21] used ^{18}O, D oxygen isotopes to study relationship between groundwater and the flow characteristics of surface water in Fuente de Piedra. Hidalgo and Cruz-Sanjulián [22] mainly studied the hydrochemical characteristics of groundwater in Norway and found that the increase in pH value of groundwater in Norway is related to the chemical characteristics of groundwater. Zhang et al. [23] studied the effects of salinity, water conductivity and dispersion on stagnation position, and level of groundwater flow system through sensitivity analysis. Previous studies also investigated the karst water chemistry characteristics and ascertained the chemical composition changes in the karst aquifer groundwater in the midwestern Kentucky of the United States [24,25]. Collins, et al. [26] conducted a study on the degree

of mineralization of groundwater and revealed that there is no obvious correlation between the degree of mineralization of groundwater and the depth of burial. In addition, the application of hydrogeochemical models is also useful in the above studies [27]. Garrels, et al. [28] proposed the normal form of the water chemistry model in the study of establishing the water chemistry model, and later proposed the water-rock interaction system based on the research. Nordstrom, et al. [29] conducted a comprehensive analysis on the main components, water quality types and corresponding trace elements of the groundwater in the Stripa area and probed into the water-rock interaction in the groundwater in the Stripa area.

Although these studies have systematically analyzed the hydro-geochemistry, groundwater cycle, and groundwater conditions of the Hetao Plain, they have some limitations in sampling, making the research on the hydrochemical distribution characteristics of the groundwater in the basin insufficiently and systematic. In addition, the highly mineralized groundwater is widely distributed in this study, while the geohydrochemical conditions are relatively complicated instead of comprehensive and systematic. Furthermore, the previous research on the formation mechanism of high mineral water mainly came from the results of speculation, which has not been systematically analyzed and investigated. This study collects the existing basic data of groundwater in the study area, and systematically analyzes the geological and hydrogeological conditions of the groundwater. These results will reveal the characteristics of the groundwater flow system and provide a scientific basis for the design of the sample data collection plan. Based on the hydrochemical analysis data of the collected groundwater samples, the traditional hydrogeochemical methods are used to qualitatively describe the spatial evolution characteristics of highly mineralized groundwater. Finally, a variety of methods (e.g., hydrochemical methods, isotope methods and hydrogeological methods) were used to systematically analyze the causes of highly mineralized water, and to reveal the formation mechanism of highly mineralized groundwater in the study area.

2. Materials and Methods

2.1. Study Area

The Hetao Plain is located in the central and western regions of the Inner Mongolia Autonomous Region (106°07′~112°15′ N and 40°10′~41°27′ E), north of the Great Wall and south of the Yinshan Mountains, from Helan Mountain in the west and east to Hohhot in the east (Figure 1). The Hetao Plain is formed by the alluvium of the Yellow River, and some of its tributaries, extending from east to west along the Yellow River, with a length of about 591.6 km, a width of 20–90 km from north to south, and an area of 23,575 km^2, are fanned out in an arc. The elevation of the study area is high in the west and low in the east. The Hetao Plain is located in an arid and semi-arid region. It is hot and humid in the summer, rainy and hot in the same period, and cold and dry in the winter with a large temperature difference between the day and night. Due to a large amount of evaporation and lack of precipitation, the agricultural water consumption in the Hetao Plain mainly comes from the Yellow River and groundwater, which is a typical irrigated agricultural region.

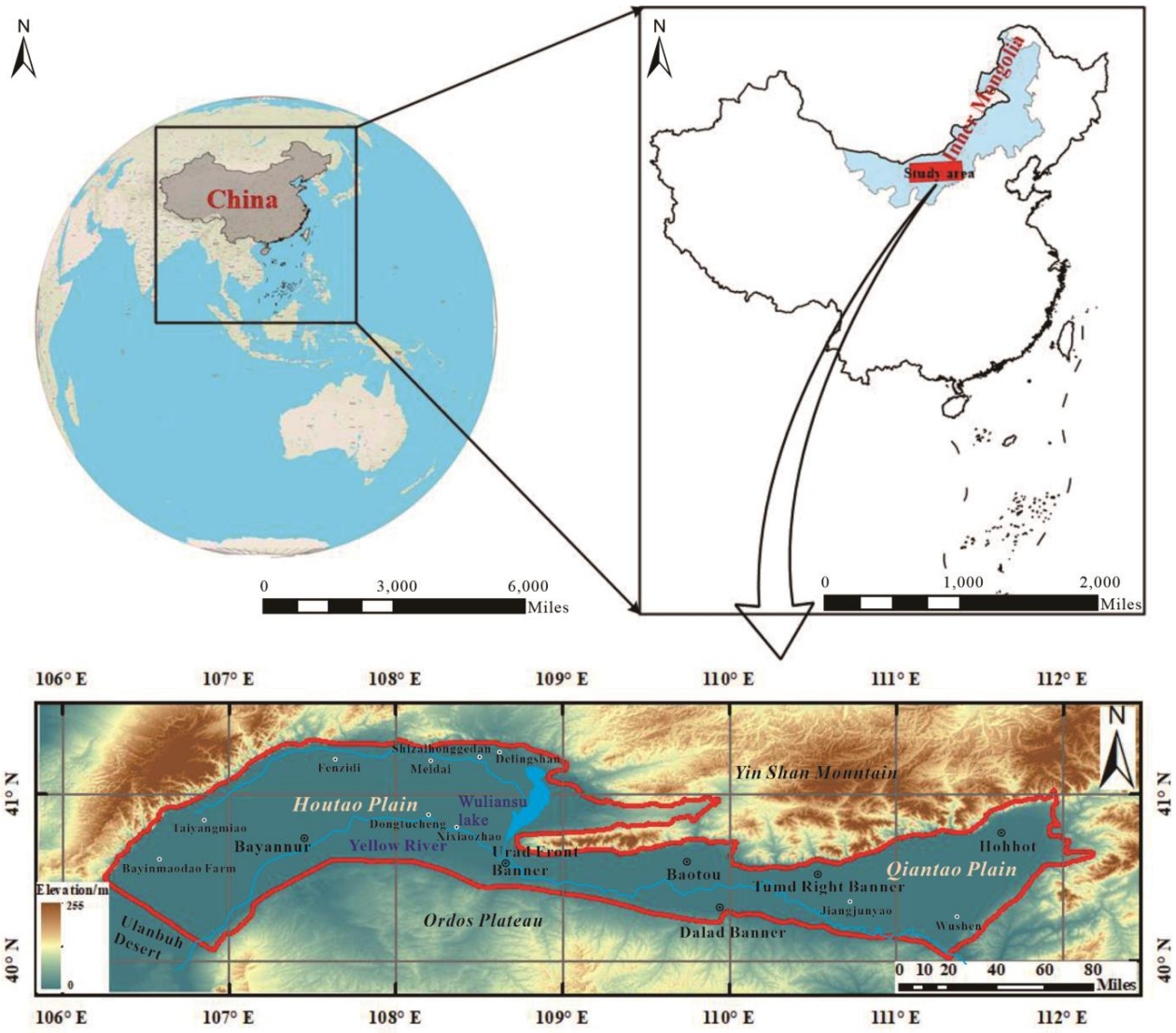

Figure 1. Geographic location and digital elevation model (DEM) of the Hetao Plain.

The study area boasts a gentle terrain, consisting of piedmont terraces, piedmont alluvial fans and alluvial plains. The study area, a large faulted basin, is located between the Yinshan Uplift and the Ordos Uplift. The stratum is dominated by Quaternary deposits, followed by Neogene, Paleogene, Cretaceous, and Jurassic, and locally are Triassic, Cambrian, Archean strata and magmatic rocks. Restricted by the sedimentary environment, the Hetao Plain has certain differences in the spatial distribution of stratigraphic lithology of different origins. Pleistocene-Holocene series are mainly gray-yellow, coarse-grained alluvial sand gravel, gravel, alluvial fine sand, medium fine sand and alluvial silt fine sand, fine sand, and interbedded silty clay; among them, alluvial-diluvial sand and gravel are not developed, and layered sodium sulfate appears in some depression areas. The Middle Pleistocene lithology is mainly composed of lake and marsh sedimentary silt, silty clay, silty fine sand and silty clay. Among them, silty clay is the most developed, widely distributed, and thick.

2.2. Principles of Sample Collection

The sampling in this study was mainly carried out when the well was in normal operation. As shown in Figure 2, the sampling density was 3–4 samples/100 km^2 at the groundwater sampling points of the regional survey and was increased in typical areas. The

survey groundwater sampling points in key areas are collected in 10–20 samples/100 km^2. During the sampling process, the number of samples collected from abnormally polluted areas is increased by 10–20%. The selection of sampling points, based on regional control, gives priority to the selection of important groundwater sources, national and provincial groundwater monitoring holes, large springs, agricultural wells, large industrial and mining enterprise-owned wells, mine drainage, oil field water supply wells, monitoring wells near important pollution sources and other well holes or water points. Sampling points in typical areas are determined by considering pollution sources, aquifer distribution, groundwater flow direction, and combining pollutant diffusion patterns. When the existing wells (springs) cannot meet the sampling density, manual exposure methods are used to collect groundwater samples.

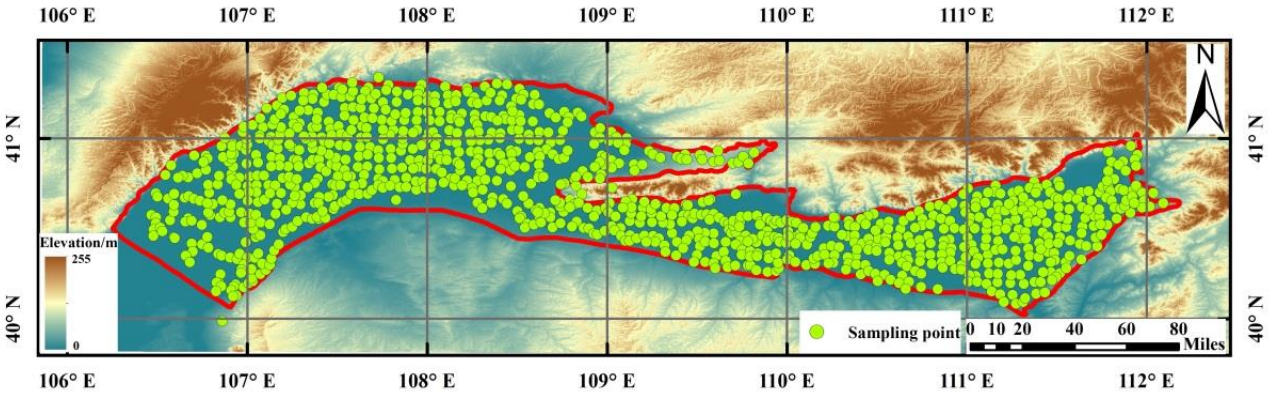

Figure 2. Spatial distribution map of groundwater sampling points in the study area.

2.3. Procedure of Sample Collection, Storage and Inspection

Before sampling, the groundwater level of the study area was measured. The sampling depth was 0.5 m below the water table. The well was pumped for 15–20 min before sampling so as to assure that the groundwater samples were fresh, and the sampling bottle was rinsed with well water 3–4 times. After sampling, 1 mL of HCL was added to the samples, and the bottle was sealed with waterproof tape. The samples were labeled and kept in cold storage at 4 °C. The samples were sent to the laboratory for testing and analysis within 7 days.

The test items for sample include total analysis, trace element analysis, δD, $\delta^{18}O$ and ^3H. The field test indexes mainly include: water temperature, pH value, electrical conductivity (EC) and dissolved total solids (TDS: Indicates how many milligrams of solid impurities are dissolved in 1 liter of water, mainly includes K^+, Na^+, Ca^{2+}, Mg^{2+}, Cl^-, SO_4^{2-}, HCO_3^-, CO_3^{2-}, etc). Briefly, concentrations of major cations (K^+, Na^+, Ca^{2+}, Mg^{2+}, Fe^{2+}, Fe^{3+}, Mn^{2+}) and trace elements were determined by inductively coupled plasma atomic emission spectrometry (ICP-AES) and inductively coupled plasma mass spectrometry (ICP-MS). The samples were analyzed for anions by ion chromatography (IC, Dionex DX-120). Arsenic concentrations in groundwater samples were determined using high performance liquid chromatography (HPLC)-ICP-MS. Fluoride and iodide were determined by ion-chromatography. The isotopic composition of $\delta^{18}O$ and δD were examined using an Isotope Ratio Mass Spectrometer (LGR LWIA-V2 (DLT-100)). The results of $\delta^{18}O$, δD were expressed in per mil unit as delta-notation relative to the Vienna Standard Mean Ocean Water (VSMOW) standard. Moreover, ^3H was tested using a low-background liquid scintillation counter.

These samples were tested by the Institute of Hydrogeology and Environmental Geology. The test ambient temperature was 23 °C and humidity was 50%. Groundwater samples were analyzed with 5% duplicates and the error of all replicates was less than 5%.

Chemical analysis for major ions have been validated using the electrical balance (E.B.) (EB% < 5%) [30], calculated applying the Equation (1):

$$EB\% = 100 \times (\Sigma cations - \Sigma anions)/(\Sigma cations + \Sigma anions) \quad (1)$$

where Σcations is the sum of cations and Σanions is the sum of anions and are measured in meq/L.

3. Results

3.1. Spatial Distribution Law of Highly Mineralized Groundwater in Hetao Plain

As shown in Figure 3, the highly mineralized water with salinity > 3 g/L is widely distributed in the shallow water-bearing layer of superficial layer in Hetao Plain, which covers an area of about 3.45 × 10^3 km^2, accounting for 11.5% of the area of Hetao Plain. In terms of the whole basin, the distribution of highly mineralized water in a horizontal direction is controlled by structural, paleogeographic, geomorphological and hydrogeological conditions, and there is an obvious horizontal zoning law. Five highly mineralized water distribution zones can be divided from west to east and from north to south: highly mineralized water distribution zone of valley in front of fan in Houtao Plain, highly mineralized water distribution zone on the north bank of Yellow River in Houtao Plain, highly mineralized water (brine) distribution zone of Xishanzui in Houtao Plain, highly mineralized water distribution zone of Hasuhai in Hubao Plain and highly mineralized water distribution zone of Dalad Banner on the south bank of Yellow River.

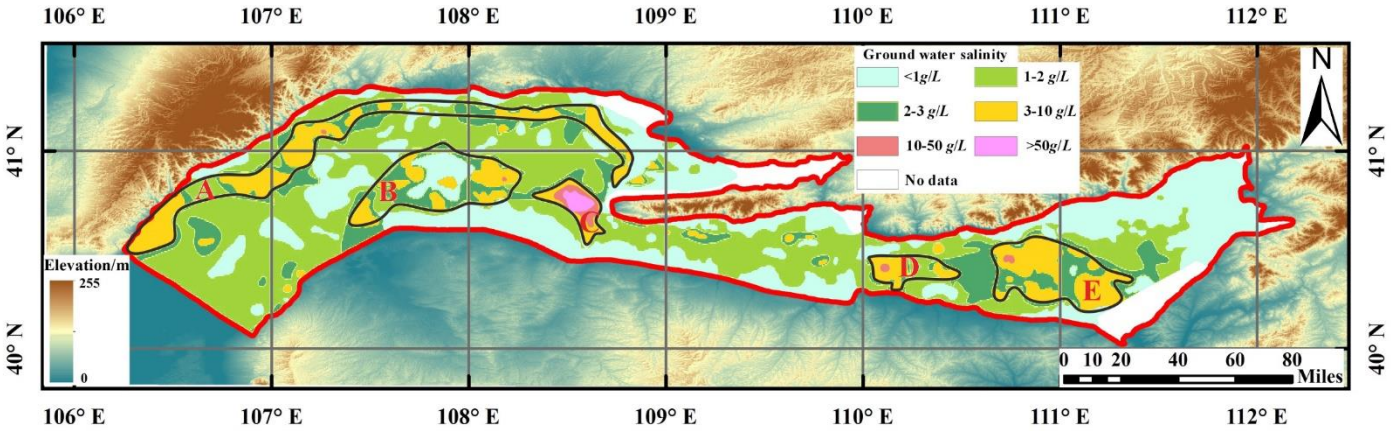

Figure 3. Distribution map of salinity in Hetao Plain. (A—Highly mineralized water distribution zone of valley in front of fan in Houtao Plain; B—Highly mineralized water distribution zone on the north bank of Yellow River in Houtao Plain; C—Highly mineralized water (brine) distribution zone of Xishanzui in Houtao Plain; D—Highly mineralized water distribution zone of Hasuhai in Hubao Plain; E- Highly mineralized water distribution zone of Dalad Banner on the south bank of Yellow River).

3.1.1. Highly Mineralized Water Distribution Zone of Valley in Front of Fan in Houtao Plain (A)

As can be seen from Figure 3, generally speaking, the salinity gradually increases from NE to SE, and then turns to SE from Shizaihonggedan to Wuliangsuhai front depression zone. The salinity increases from 3.0 g/L to 9.2 g/L, and the east side of Wuliangsuhai is the high value area of salinity in this area. The saline water belt is distributed on the south side of valley at the front edge of the fan skirt in front of Langshan Mountain, which runs through the north of the whole region from west to east, with a length of over 180 km from east to west and an average width of 2~10 km from north to south. The widest belt distributed in Taiyangmiao Township-Fenzidi Township is 3.5~13.8 km; in the west of Gucheng Township, it is located on the north edge of Ulan Buh Desert on the south side

of the main drainage trunk; in the east of Gucheng Township, it is distributed along both sides of the main drainage trunk and extends eastward to the west side of Wuliangsuhai. It is staggered with the fresh water belt on the north side in canine shape. In the direction of the fan axis of the larger alluvial-proluvial fan, fresh water extends farther south, while in the wing of the fan group, salt water extends northward. Due to the hydrodynamic differentiation, the salinity of the saline water zone tends to increase from west to east. At the same time, due to the desalination of fresh water from large alluvial-proluvial fans, the saline water zone is unevenly distributed, which can be roughly divided into 4 sections, and the water quality in the east section is especially salty. From west to east, the first section from Bayinmaodao Farm to Taiyangmiao Farm is distributed in NE-SW direction, with a narrow width of 3–5 km in general. Most of them are Cl-Na and Cl•SO_4-Na water with salinity of 4.0~4.4 g/L, and the local salinity is high, with the highest point reaching 9.4 g/L. The second section is located in Taiyangmiao Township-Fenzidi Township, which is the longest saline water belt in the whole region, and also distributed in NE direction. Most of them are Cl•SO_4-Na and Cl•SO_4-Na•Mg type water with salinity of 3.0~8.2 g/L, and the local salinity is greater than 16 g/L. The third section is located in the northwest of Meidai Township-Shizai Honggedan area, distributed in west-east direction, with salinity ranging from 3.4 g/L to 7.7 g/L, and mainly composed of Cl•SO_4-Na•Mg type water and Cl•HCO_3-Na•Mg type water. The fourth section is located from the south of Delingshan Township to the west of Wuliangsuhai, distributed in the south-east direction, with the salinity increasing to 6.4~9.2 g/L, and mainly composed of Cl•SO_4-Na•Mg and Cl•HCO_3-Na•Mg type water.

3.1.2. Highly Mineralized Water Distribution Zone on the North Bank of Yellow River in Houtao Plain (B)

Highly mineralized water is mainly distributed around Dongtucheng Village, along the north and south sides of the main canal. It is narrow in the west and wide in the east, generally about 5–15 km wide. Due to the influence of complex agricultural irrigation and canal system leakage on the surface, it is distributed in intermittent round or oval patches with irregular size and shape, totaling as many as six patches. Among them, the largest area distributed around Bayantaohai Town is 180 km^2, and Cl-Na, Cl•SO_4-Na and Cl•SO_4•HCO_3-Na with salinity of 1.1–7.2 g/L are the main types.

3.1.3. Highly Mineralized Water (Brine) Distribution Zone of Xishanzui in Houtao Plain (C)

Highly mineralized water is mainly distributed from Xixiaozhao Township to the early Urad period, and is elliptical along the north side of the main canal in NW-SE direction, with a long axis of 23.5 km and a short axis of about 12.9 km. This area is the saline water belt with the highest salinity in the whole Hetao Plain. Its salinity is generally greater than 10 g/L, and tends to increase from the periphery to the oval center, especially in Luguanhao Village, where the salinity is the highest and the water quality is the saltiest, reaching 70.0 g/L. The hydrochemical types are mainly Cl-Na and Cl•SO_4-Na type water.

3.1.4. Highly Mineralized Water Distribution Zone of Hasuhai in Hubao Plain (D)

Highly mineralized water is distributed in the alluvial plain of the Yellow River. It is in the shape of tadpoles with wide north and narrow south. Most of them are HCO_3-Na, HCO_3•SO_4•Na and Cl•SO_4-Na with salinity of 2.9~7.2 g/L, and only in the northwest of Dongba Village. In addition, from the piedmont sloping plain area, transition area to the alluvial plain area on the south bank of the Yellow River, the change in groundwater salinity represents a certain law: from south to north, and from west to east, the salinity gradually increases, and the water quality gradually becomes salty.

3.1.5. Highly Mineralized Water Distribution Zone of Dalad Banner on the South Bank of Yellow River (E)

Highly mineralized water is mainly distributed on the impact plain of the Yellow River and Dahei River in the southwest of Hubao Plain, bounded by the depression in front of Langshan Mountain in the north, the north bank of the Yellow River in the south, Jiangjunyao Township in the west, and extending eastward to Wushen Township. The hydrochemical types are complex, mainly Cl•SO_4•HCO_3-Na•Mg and HCO_3•Cl-Na•Mg type water. The distribution zone of highly mineralized water on the south bank of the intersection of Dahei River and Shilawusu River extends far to the southeast. The chemical characteristics of groundwater show that the salinity of groundwater increases continuously from northeast to southwest along the direction of groundwater runoff, and gradually transits from fresh water to brackish water and saline water. As a result, the water quality gradually deteriorates.

3.2. Spatial Distribution Law of Highly Mineralized Groundwater in Hetao Plain

3.2.1. Correlation between Salinity and Major Ions

According to Table 1, the correlation coefficients between salinity and the main cations Mg^{2+} and Na^{+} in five highly mineralized water distribution zones in the basin are all above 0.83, showing a high correlation, while the correlation between salinity and cations Ca^{2+} is slightly worse, showing a significant correlation. There is a weak correlation between salinity and Ca^{2+} in the highly mineralized water distribution zones on the south bank of the Yellow River in Dalad Banner and the north bank of the Yellow River in Houtao Plain. The five highly mineralized water distribution zones are highly correlated with the main anion Cl^{-}, and the correlation coefficients are all above 0.81. Except for the highly mineralized water distribution zone in the front fan depression of Houtao Plain, the correlation coefficients of the other four highly mineralized water distribution zones for the anion $SO_4{}^{2-}$ are between 0.60 and 0.99, showing a significant to high correlation. However, for $HCO_3{}^{-}$, the correlation is weak. The main reason for the above correspondence between salinity and main ions is that the solubility of salts in water is different. Generally speaking, the solubility of chloride salt is the highest, followed by sulfate and carbonate. Calcium sulfate, especially calcium and magnesium carbonate, has the smallest solubility. With the increase in salinity, the carbonate of calcium and magnesium first reaches saturation and precipitates, and when the salinity continues to increase, the sulfate of calcium also saturates and precipitates, so the soluble chlorine and sodium are dominant in highly mineralized water.

Table 1. Correlation between main chemical components of groundwater and TDS in highly mineralized water distribution zone.

	A	B	C	D	E
Ca^{2+}	0.670	0.393	0.746	0.093	0.834
Mg^{2+}	0.831	0.984	0.927	0.918	0.941
Na^{+} + K^{+}	0.945	0.994	0.996	0.991	0.997
Cl^{-}	0.946	0.997	0.997	0.815	0.986
$SO_4{}^{2-}$	0.156	0.945	0.791	0.994	0.608
$HCO_3{}^{-}$	−0.324	−0.054	−0.057	0.489	−0.101
Br^{-}	0.810	0.810	0.930	−0.019	0.953
I^{-}	0.638	0.898	0.678	0.904	0.819
F^{-}	−0.024	0.413	−0.154	0.371	−0.094
Fe^{3+}	0.142	0.307	−0.264	0.165	−0.119
Fe^{2+}	0.411	0.428	−0.354	0.002	−0.043
As	0.299	−0.079	−0.596	−0.173	−0.145

The correlation coefficients between salinity and I-in five highly mineralized water distribution zones are all above 0.63, showing significant and high correlation; the correlation coefficient with Br- is high except the distribution zone of highly mineralized water in

Dalad Banner on the south bank of the Yellow River, showing a high correlation, except that the distribution zone of highly mineralized water in Xishanzui of Houtao Plain has significant negative correlation with As (that is, the higher the salinity, the lower the arsenic content). The distribution zone of highly mineralized water in front depression of Houtao Fan has a low correlation with Fe^{2+}, and the correlation with As, arsenic, F^{-}, Fe^{3+} and Fe^{2+} is weak. In a certain sense, this indicates that the source and genesis of I^{-} in shallow groundwater in the basin are similar to those of TDS.

In conclusion, according to Figure 4, the main cations are Mg^{2+} and Na^{+}, and the main anions are Cl^{-} and $SO_4{}^{2-}$ in the highly mineralized water distribution zone in the basin, and the content of I^{-} in groundwater in the highly mineralized water distribution zone is also high.

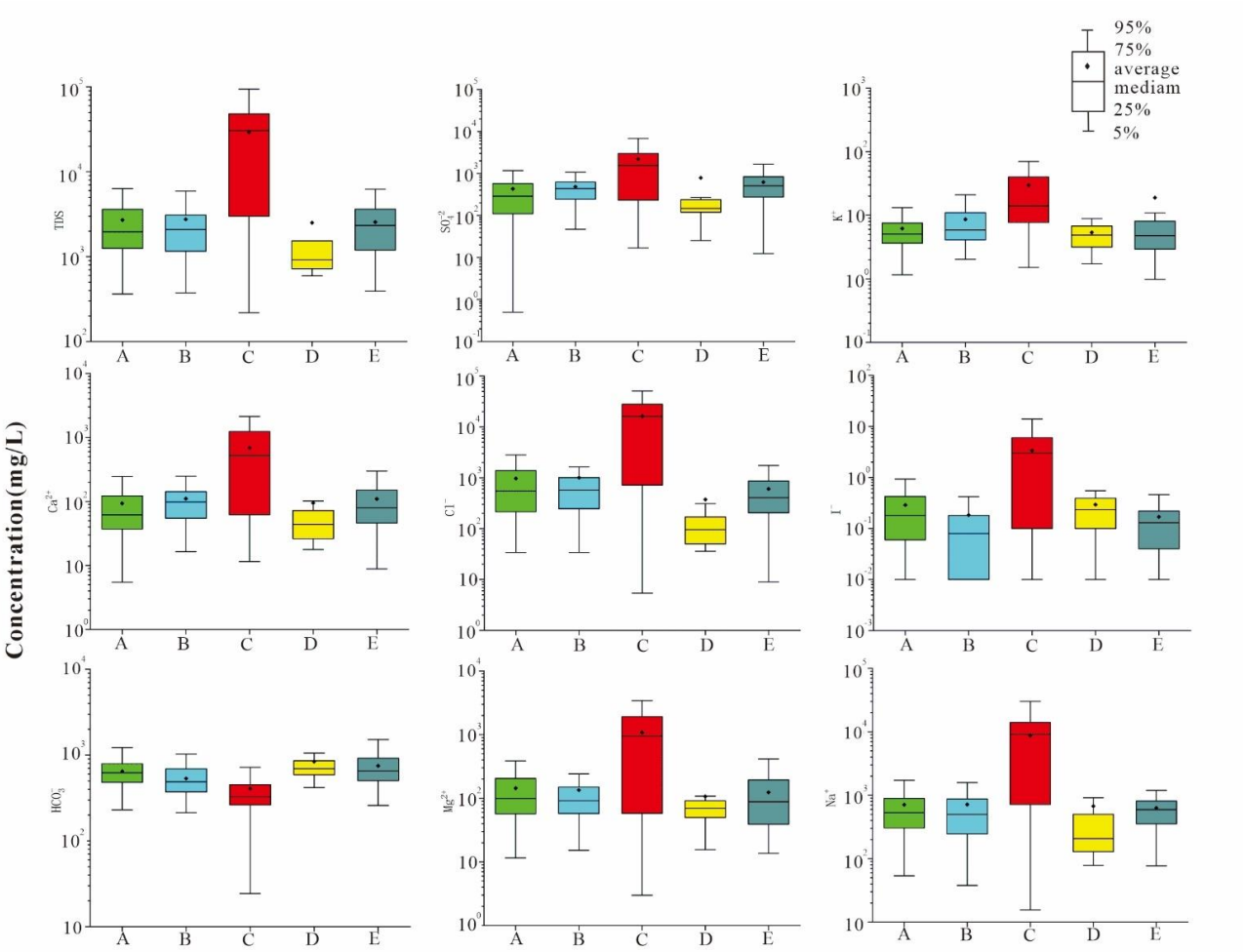

Figure 4. Box plot of TDS and the main ion concentrations in the five zones according to the map in Figure 3.

3.2.2. Analysis Based on Three-Line Diagram (Piper)

It can be seen from the three-line diagram (Figure 5) that in the cation triangle diagram, several samples in the distribution zone of highly mineralized water show similar trends, and cations develop in the direction of increasing the relative content of Na + K. On the anion triangle diagram, the distribution of anions in several highly mineralized water distribution zones is more dispersed than that of the cations. The content of Cl^{-} is relatively increased, but except for the highly mineralized water distribution zone in Houtao Plain, the falling points of anions in other highly mineralized water distribution zones are all between Cl^{-} 35% and 80% on the three-line diagram. A small part of Cl^{-} in the sample points of the highly mineralized water distribution zone in Xishanzui in Houtao Plain falls

in this area, and most of it falls outside this range with its content close to 100%. Finally, from the diamond chart, the distribution zones of highly mineralized water have basically the same hydrochemical evolution trend. All of them are transformed into Cl • SO_4-Na • Mg and Cl-Na • Mg type water, while the anomalous falling point of the highly mineralized water in Xishanzui of Houtao Plain is the same as that of anions (i.e., the highly mineralized water mainly composed of Cl-Na type water), which indicates that the highly mineralized water in Xishanzui of Houtao Plain is different from other highly mineralized zone water sources.

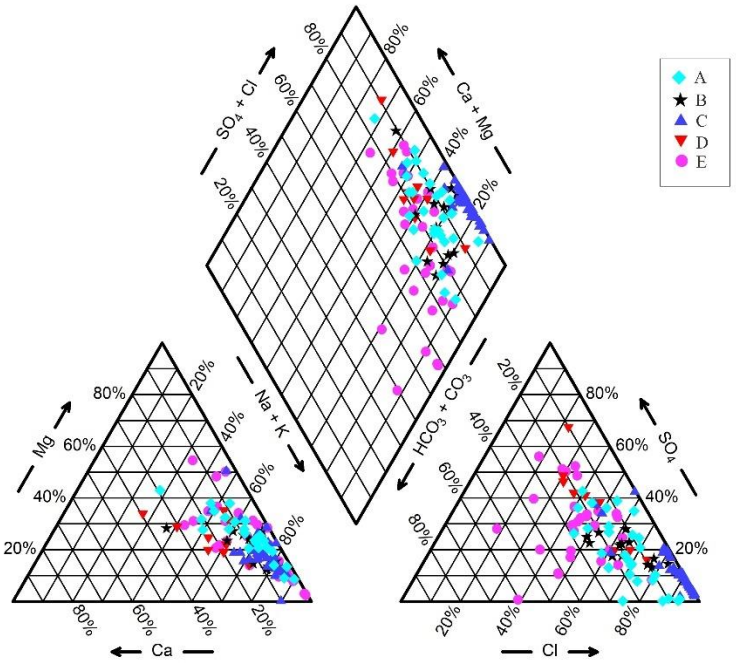

Figure 5. Three-line diagram of highly mineralized water distribution zone in Hetao.

4. Discussion

The chemical composition in groundwater is formed through a long geological historical process. In the process of its formation, although affected by many factors, such as various rock (soil) properties, hydrogeological conditions, groundwater circulation conditions, climate and others, various complex physical and chemical reactions will occur, and its chemical composition still has certain inheritance to the chemical composition of the origin water. Therefore, the study on the chemical composition of groundwater and identification of its origin can inverse the formation and evolution process of highly mineralized water. The shallow groundwater in Hetao Plain originated from leaching-infiltration water, while deep groundwater originated from sedimentary-buried water (continental origin). The groundwater of continental sedimentary origin is buried in the depth of several hundred meters or even several kilometers below the surface of the earth and has no or basically no hydraulic connection with infiltration water of atmospheric origin. Therefore, the study on hydrogeochemical characteristics of groundwater of two different origins is helpful for understanding the origin of shallow highly mineralized water in Hetao Plain. At the same time, the groundwater of continental sedimentary origin has the hydrogeochemical characteristics similar to that of marine sedimentary origin (i.e., high salinity, main ions are Cl^-, Na^+, and there are more trace elements such as Br and I). Therefore, it is possible to study continental sedimentary groundwater by studying the hydrochemistry of marine sedimentary groundwater. In the following description, "seawater or marine sedimentary groundwater" will be used to replace the deep groundwater of continental sedimentary origin in Hetao basin for convenience of understanding. At present, the Gibbs diagram and content ratio coefficient among various components are often used as important basis for

studying groundwater hydrogeochemistry in marine sediments. The following methods are used to analyze the main formation of chemical components of highly mineralized water in Hetao Plain.

4.1. Indication of Geochemical Indicators

4.1.1. Analysis Based on Gibbs Diagram

In order to compare the chemical composition, formation reasons and relationship between surface water and groundwater intuitively, Gibbs designed a semi-logarithmic coordinate function to simply and effectively judge the relative importance of various ion origin mechanisms (precipitation-controlled, rock weathering-controlled and "evaporation-concentration") in surface water or groundwater by using the relationship between $Cl^-/(Cl^- + HCO_3^-)$ and TDS or the relationship between $Na^+/(Na^+ + Ca^{2+})$ and TDS. Then, a Gibbs diagram is made with the water quality data of sampling points in five highly mineralized water distribution zones in Hetao Plain (Figure 6), and the ionic chemical characteristics of each highly mineralized water distribution zone are analyzed.

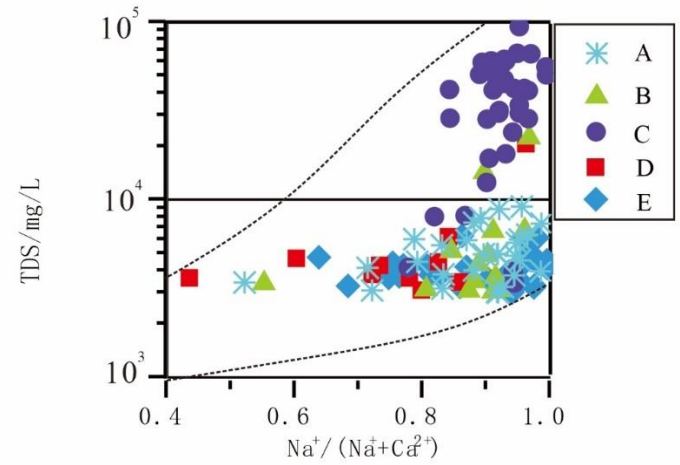

Figure 6. Gibbs diagram of sampling points in different highly mineralized water distribution zones in shallow Hetao Plain.

In the Gibbs diagram (Figure 6), except for the discreteness of the samples located in Xishanzui highly mineralized water distribution zone in Houtao Plain, the hydrochemical characteristic values of the other five highly mineralized water distribution zones are concentrated in the dotted line range, all of which fall within the range of $Na^+/(Na^+ + Ca^{2+})$ greater than 0.5, indicating that their ionic components mainly come from evaporation-concentration process. The $Na^+/(Na^+ + Ca^{2+})$ ratio of about 50% samples in Xishanzui highly mineralized water distribution zone of Houtao Plain is >0.9, which indicates that the groundwater in this zone is recharged by groundwater from marine sediments, namely, deep groundwater recharge.

4.1.2. The $\gamma(Na^+)/\gamma(Cl^-)$ Coefficient

According to its origin, characteristics and distribution, water in nature can be divided into continental fresh water, ocean seawater and groundwater. Groundwater is actually water preserved in sediments by continental freshwater or oceanic seawater of different ages. Therefore, according to the formation environment, water can be divided into two categories: continental fresh water and marine water.

The $\gamma(Na^+)/\gamma(Cl^-)$ coefficient is a hydrogeochemical parameter that characterizes the enrichment degree of sodium ions in groundwater. The average $\gamma(Na^+)/\gamma(Cl^-)$ coefficient of standard seawater is 0.85. Continental freshwater has a higher $\gamma(Na^+)/\gamma(Cl^-)$ coefficient $\gamma(Na^+)/\gamma(Cl^-) > 0.85$, while oceanic seawater has a lower $\gamma(Na^+)/\gamma(Cl^-)$ coefficient $\gamma(Na^+)/\gamma(Cl^-) < 0.85$ [31].

The relationship between $\gamma(Na^+)/\gamma(Cl^-)$ coefficient of sampling points of five highly mineralized water distribution zones in shallow groundwater of Hetao Plain and $\gamma(Na^+)/\gamma(Cl^-)$ coefficient of standard seawater is shown in Figure 7. It can be seen from the figure that the $\gamma(Na^+)/\gamma(Cl^-)$ values of groundwater in Hasuhai of Hubao Plain and Dalad Banner on the south bank of Yellow River are higher than 0.85. It shows that Na^+ and other basic ions in shallow groundwater mainly come from the dissolution of silicate minerals, and groundwater does not originate from modern seawater or marine sedimentary water, that is, it is not formed by deep brine infection and jacking recharge along faults and uplift structures. Therefore, the salinity of groundwater in these highly mineralized water distribution zones is relatively high, which may be mainly affected by climate, sedimentary environment, hydrogeological conditions, hydrology and other factors.

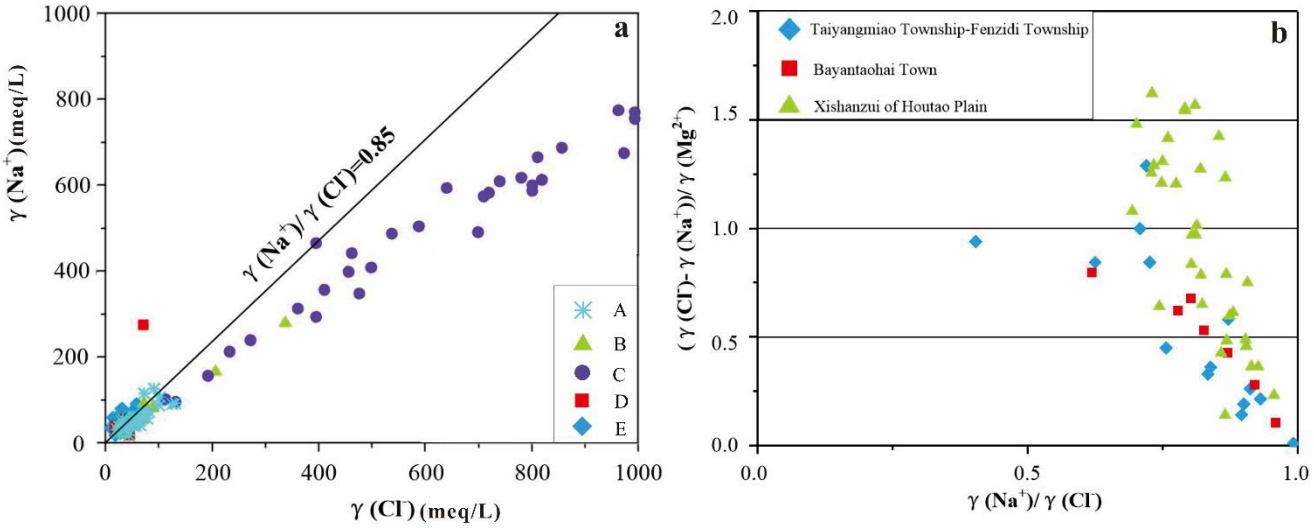

Figure 7. The $\gamma(Na^+)/\gamma(Cl^-)$ scale coefficient (**a**) and relationship between $\gamma(Na^+)/\gamma(Cl^-)$ and $(\gamma(Cl^-)\text{-}\gamma(Na^+))/\gamma(Mg^{2+})$ diagram (**b**) of shallow groundwater in Hetao Plain.

However, the $\gamma(Na^+)/\gamma(Cl^-)$ values of some samples in the pre-fan depression, the north bank of the Yellow River and Xishanzui highly mineralized water distribution zone of Houtao Plain are lower than 0.85, and 22% of the samples in the highly mineralized water distribution zone in the pre-fan depression of Houtao Plain are lower than 0.85, mainly distributed in the second highly mineralized water distribution zone of this zone (namely Taiyangmiao Township-Fenzidi Township); 8% of the samples in the highly mineralized water distribution zone on the north bank of the Yellow River in Houtao Plain have $\gamma(Na^+)/\gamma(Cl^-)$ value lower than 0.85, which is mainly distributed in the highly mineralized water area of Bayantaohai Town in the east of the zone; 90% of samples in Xishanzui highly mineralized water distribution zone in Houtao Plain have $\gamma(Na^+)/\gamma(Cl^-)$ value lower than 0.85. From the above analysis, we can draw a preliminary conclusion that the groundwater in these three highly mineralized water areas be recharged by groundwater of deep marine sedimentary origin.

The above conclusions are only obtained by a simple analysis of the $\gamma(Na^+)/\gamma(Cl^-)$ coefficient. The Sulin's classification method is introduced to further analyze the causes of highly mineralized water in Taiyangmiao Township-Fenzidi Township, Bayantaohai Town on the north bank of the Yellow River and Xishanzui bittern water zone in Houtao Plain so that the correctness of this conclusion can be further verified

According to Sulin's classification that $\gamma(Na^+)/\gamma(Cl^-) < 1$, $(\gamma(Cl^-)\text{-}\gamma(Na^+))/\gamma(Mg^{2+}) > 1$ belongs to calcium chloride water, and that this type of groundwater is in deep environment [32]. The analysis results of highly mineralized water samples in Taiyangmiao Township-Fenzidi Township, Houtao Plain Fan Front Depression, Xishanzui Brine Belt

and Bayantaohai Town of Houtao Plain according to Sulin's Classification are shown in Figure 7.

It can be seen from the Figure 7 that the $\gamma(Na^+)/\gamma(Cl^-)$ mass of the three highly mineralized water distribution zones are all less than 1, meeting the first condition of Sulin's classification, while the values of $(\gamma(Cl^-)\text{-}\gamma(Na^+))/\gamma(Mg^{2+})$ in Taiyangmiao-Fenzidi Township and Bayantaohai Town are all less than 1, which does not completely meet the second limit condition of Sulin's classification. The value of 55% samples in Xishanzui brine area of Houtao Plain is greater than 1, basically meeting the second condition of Sulin's classification. Therefore, it can be further concluded that the brine in Xishanzui highly mineralized water distribution zone of Houtao Plain may come from deep brine.

4.1.3. The Saturation Indexes of the Main Minerals

The equilibrium state of water with respect to a particular mineral phase can be determined by calculating the saturation index (*SI*), using chemical data to distinguish the hydrogeochemical evolution as well as by identifying the geochemical reactions that control the water chemistry. Using the geochemical software PHREEQC, *SI* was computed the ion activity product (IAP), which was compared to the solubility product (Ksp; Equation (2)). [33,34]. If *SI* is greater than zero, it indicates an oversaturation (precipitation) of a particular mineral. If it is less than zero, it reveals an unsaturation (dissolution) of a concerned mineral. If it is equal to zero, it indicates the saturation (equilibrium) of a particular mineral.

$$SI = \frac{K_{IAP}}{K_{SP}} \quad (2)$$

We calculated the *SI* of groundwater in area C, where the groundwater salinity is highest. According to the calculation, the obtained *SI* vs. TDS dependences is shown in Figure 8. The *SI* variation range of dolomite, calcite, gypsum and halite is, respectively: −1.2~3.4, −9.7~1.45, −1.54~0.12, −4.72~−1.55. Gypsum and halite $SI < 0$, and the aquifer sediments in this area are rich in rock salt and gypsum, so the contribution of these two minerals in groundwater ions is absolutely dominant. The *SI* of calcite and dolomite is mostly positive and close to 0, indicating that these two minerals are most likely present in the aquifer environment and control the chemical composition of the groundwater.

4.1.4. Relationship between γ (Ca^{2+} + Mg^{2+}) and γ (SO_4^{2-} + HCO_3^-)

Fisher and Mullican think that if Ca^{2+}, Mg^{2+}, SO_4^{2-} and HCO_3^- in groundwater only come from the dissolution of calcite, dolomite and gypsum, there will be a good balance between anions and cations in water [35]. However, when seawater invades freshwater water-bearing layer, this balance will be destroyed by the reverse exchange reaction between Na^+ and Ca^{2+} ions.

The sample points of the other four highly mineralized water zones in Hetao Plain (except Xishanzui of Houtao Plain) are all distributed on or near diagonal lines in the maps drawn by γ (Ca^{2+} + Mg^{2+}) and γ (SO_4^{2-} + HCO_3^-) (Figure 9), that is, there is a good balance relationship among Ca^{2+}, Mg^{2+}, SO_4^{2-} and HCO_3^- in groundwater. It is further inferred that the groundwater formation of these highly mineralized water zones is leaching-infiltration water. Most of the sample points in Xishanzui highly mineralized water belt of Houtao Plain deviating from 1:1 diagonal, γ (Ca^{2+} + Mg^{2+}) was significantly higher than γ (SO_4^{2-} + HCO_3^-). According to Fisher and Mullican [35]: The emergence of this phenomenon, given that the water-bearing layer is infected by seawater, the Na^+ in seawater is much higher than that in fresh water, and the exchangeable cations on the surface of fresh water water-bearing layer particles are mainly Ca^2. The reverse exchange reaction between Na^+ in seawater and Ca^{2+} on the surface of particles will occur, resulting in the increase in Ca^{2+} concentration in groundwater, which will lead to the destruction of the equilibrium system of Ca^{2+}, Mg^{2+}, SO_4^{2-} and HCO_3^- in groundwater. Therefore, it can be concluded that the brine in Xishanzui highly mineralized water zone of Houtao Plain was infected by deep underground brine.

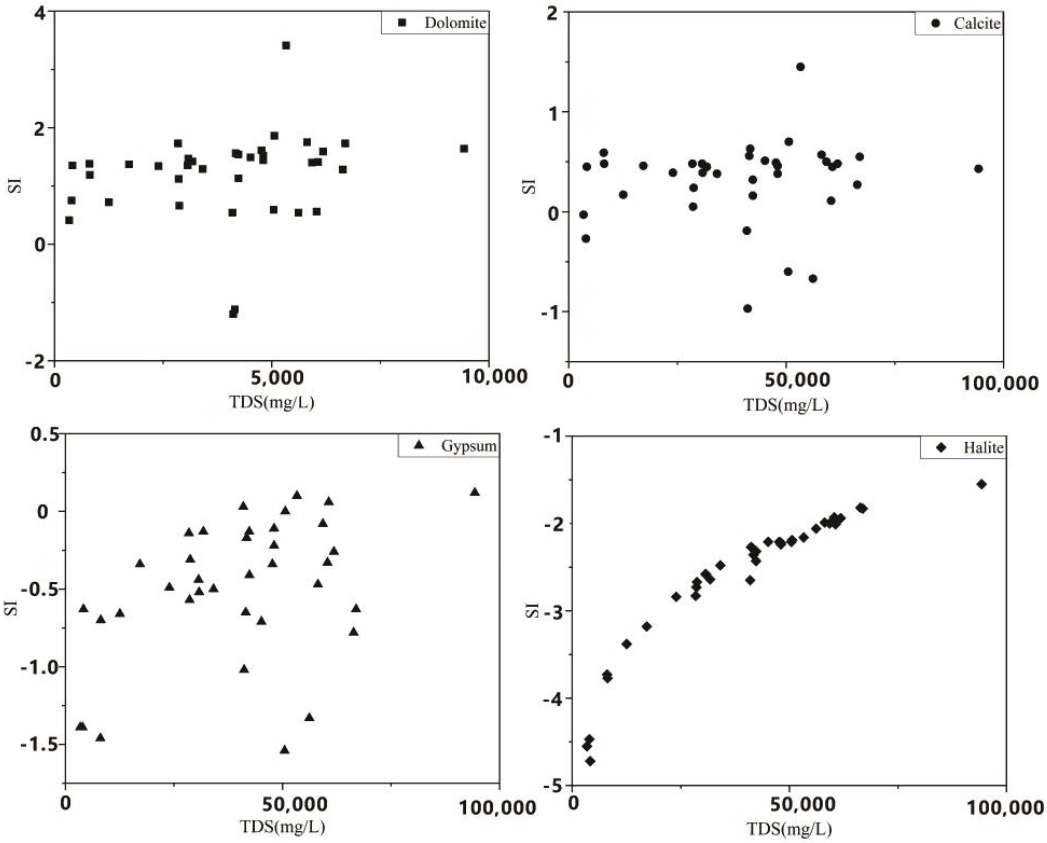

Figure 8. Relations between saturation indices and TDS of the four minerals.

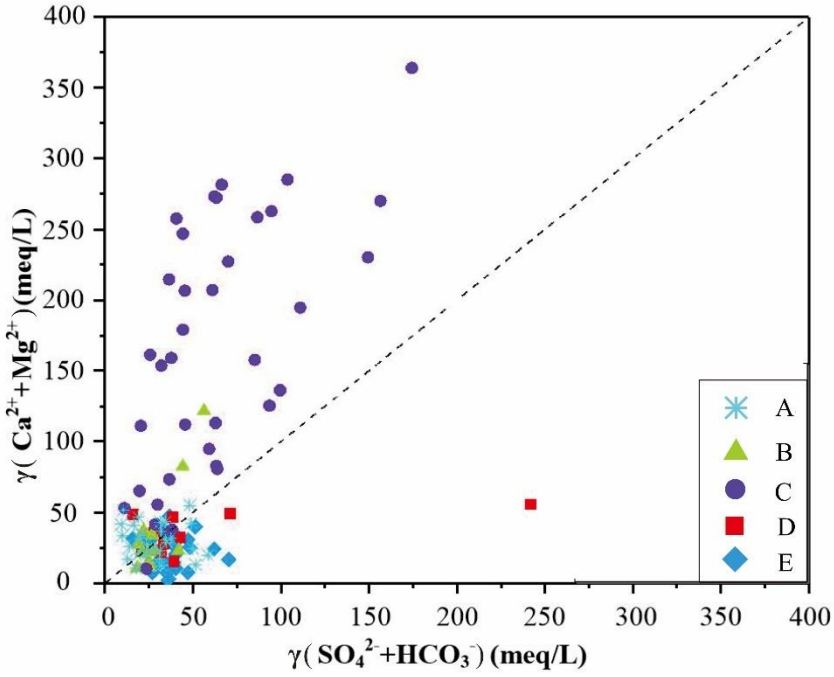

Figure 9. Relationship between γ (Ca^{2+} + Mg^{2+}) and γ (SO_4^{2-} + HCO_3^-) in shallow groundwater of Hetao Plain.

4.2. Isotopic Indication of the Origin of Xishanzui Brine

4.2.1. Oxygen Isotope Indication

The δ^{18}O-TDS relationship is usually used to identify evaporation, salt dissolution, and salt water mixing. Generally, the δ^{18}O value of groundwater salinity caused by evaporation varies greatly, while the salinity degree varies little. The sample points are distributed along the δ^{18}O axis, with a slight shift [36]. The solid points in the figure represent groundwater samples with salinity are greater than 20 g/L, and the hollow points represent brassy water and fresh water samples with salinity are less than 2 g/L. The variation of δ^{18}O in salinity caused by groundwater dissolved salts is small, and the sample points are distributed along the TDS axis. The δ^{18}O value of salt water diluted by fresh water will increase with the increase in salinity. Figure 10 shows the δ^{18}O-TDS relationship of samples with different salinity in the distribution area of high salinity water in Xishanzui. It can be seen that the highly mineralized samples are roughly distributed along a straight line between fresh water and brine 27 sample with the highest salinity (90 g/L), indicating that the shallow highly mineralized groundwater has experienced the influence of freshwater mixing dilution.

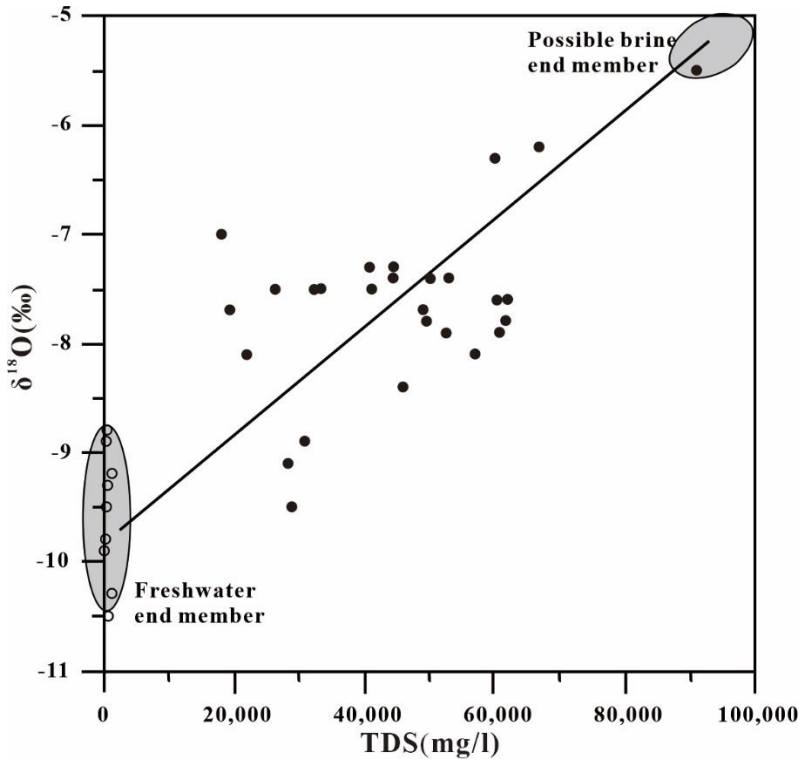

Figure 10. δ^{18}O-TDS value relationship of subsurface brine in Xishanzui.

4.2.2. Chlorine Isotope Indication

The chlorine isotope standard was standard sea water, and the δ^{37}Cl value was 0, compared with 0.0 ± 0.01‰ in modern sea water. The range of δ^{37}Cl in atmospheric solutions is known to be +0.42‰~2.53‰. The δ^{37}Cl of river water is higher with the range from +0.74‰ to +2.85‰, while the δ^{37}Cl of salt lake brine is lower and with the range from −2.06‰ to +1.01‰. Theδ^{37}Cl of groundwater varies from −0.50‰ to +0.69‰, and the δ^{37}Cl of rock salt varies from −0.6‰ to +1.2‰ [37].

The δ^{37}Cl values of underground brine in Xishanzui vary widely, with the range from −0.02‰ to 3.43‰, and most of them range from 0‰ to 2‰ (Figure 11). Except for one sample, the δ^{37}Cl values are almost greater than 0‰. Such a wide range of chlorine isotope composition indicate that is not a single underground brine of salt source, but there are multiple sources and severe isotope shunt effect, reflecting that this is an active system. As

for the existing various mixing, leached, and especially this kind of shallow underground brine, make-up water mixture is often unavoidable.

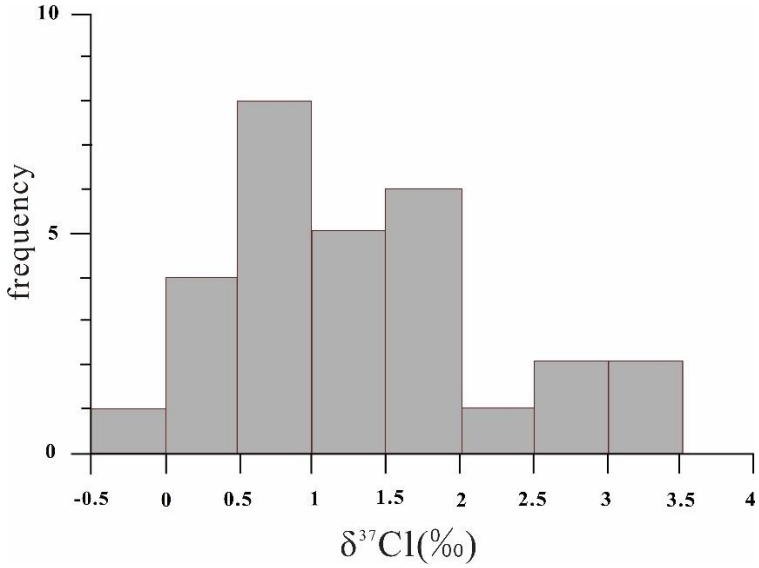

Figure 11. Sample distribution frequency of chlorine isotopic composition in Xishanzui brine.

Among the samples, the highest frequency of occurrence ranges from 0.5‰ to 1.0‰, which overlaps with the variation range of $\delta^{37}Cl$ in salt sediments, indicating that chlorine in samples with $\delta^{37}Cl$ values less than 1.0‰ mainly comes from the dissolution of salts. Delta $\delta^{37}Cl$-$\delta^{18}O$ value relationship shows that the delta delta $\delta^{37}Cl$ samples of Cl value is less than 1.0 ‰ of the delta values of $\delta^{18}O$ (namely, 7.1‰, 9.5‰, and the average to 8.1 ± 0.7‰), that the delta 37 samples of Cl value is greater than 1.0 ‰ (was 5.5‰, 9.2‰, the average to 7.4 ± 0.9‰), and that the former is lower than modern atmospheric precipitation, and may represent older groundwater (Figure 12a).

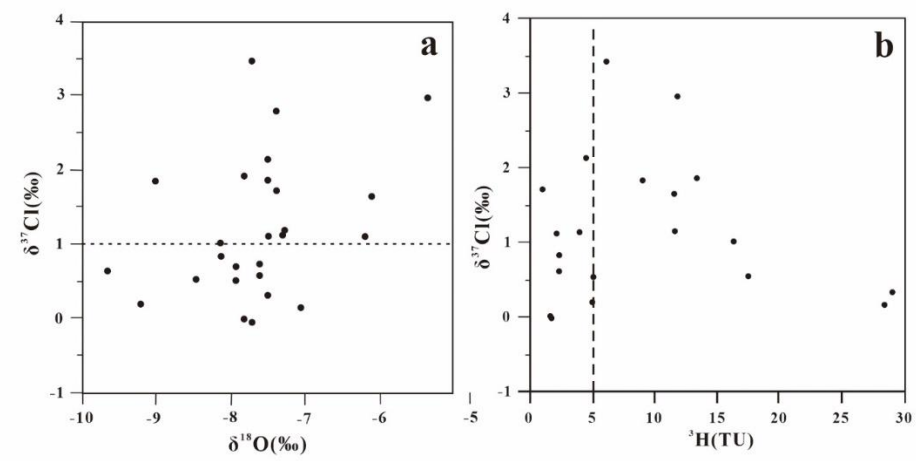

Figure 12. $\delta^{37}Cl$-$\delta^{18}O$ (**a**) and $\delta^{37}Cl$-^{3}H (**b**) value relationship of subsurface brine in Xishanzui.

Generally, in the process of rock salt crystallization and precipitation, $\delta^{37}Cl$ preferentially enters the salt sediment, resulting in the relative dilution of $\delta^{37}Cl$ in the co-existing water. With the continuous enrichment of $\delta^{37}Cl$ in salt minerals, $\delta^{37}Cl$ continues to be depleted in the brine, while the $\delta^{37}Cl$ value of the brine gradually decreases. The $\delta^{37}Cl$ value of a carnallite in Qaidam Basin, Qinghai Province is 24.7 ± 2.9‰, while the $\delta^{37}Cl$ value of brine is −0.6 ± 1.4‰, indicating that $\delta^{37}Cl$ is highly enriched during carnallite crystallization [38]. Therefore, due to the high $\delta^{37}Cl$ in precipitation and river water, the

terrestrial evaporites in the groundwater filtration formation fed by modern precipitation and surface river water will lead to the enrichment of $\delta^{37}Cl$ in brine water.

According to Figure 12b, the relationship between ^{3}H content and $\delta^{37}Cl$ value of subsurface brine samples in Xishanzui, it can be seen that the highest $\delta^{37}Cl$ value appears in the samples with obvious presence of modern water ($^{3}H > 5TU$), and the $\delta^{37}Cl$ value in these modern water samples tends to decrease with the increase in ^{3}H content. Figure 12b shows that the sample of Xishanzui underground brine contains modern water ($^{3}H > 5TU$); it can be seen that the tritium content increases with the increase in the sampling depth. Based on the simple piston flow model, the age of groundwater may be from recent years, somewhere between 20–30 years. Therefore, the brine samples with high $\delta^{37}Cl$ value are obviously affected by modern water.

4.3. The Origin of Underground Brine

The characteristic values of hydrogen and oxygen stable isotopes of water isotopes in the Yellow River and the relationship lines of water isotopes in the Yellow River were quoted from the test data of Gao et al. [39] on 10 points above Toudaoguai in Tuoketo County, Inner Mongolia (average: −10.5‰, −78.4‰). The atmospheric precipitation and its average value were obtained from the precipitation monitoring data of IAEA Baotou monitoring station.

As can be seen from Figure 13a, the variation range of stable isotopes in underground fresh water is small. Most of the samples fall to the lower left of the precipitation line (except some points), which is much smaller than the average value of local precipitation, and close to the average value of Yellow River water, indicating that Yellow River water is recharge but boasts absolute advantage in underground fresh water. The δ-value of underground brine is obviously higher than that of underground fresh water, reflecting the different recharge conditions between them. The samples of underground brine water fall in the upper right of underground fresh water. Most of them are lower than the average value of atmospheric precipitation, but much higher than the average value of Yellow River water, indicating that the recharge source of underground brine water is not closely related to the Yellow River and the local atmospheric precipitation. The variation range of δ-value of isotope of underground brine water is large, indicating that the source of recharge water is not single, nor is it affected by different types of water during the migration process. The groundwater containing tritium falls near the isotope line of Yellow River, indicating that it is affected by the underground fresh water replenished by Yellow River. The slope of the fitted line is almost the same as that of the modern local meteoric water line, but the deuterium excess is relatively small, with an average value of −6. The mean value of Baotou meteoric water to excess is 8.3.

Deuterium excess (Dxs) is defined as: $d = \delta D\text{-}8\delta^{18}O$, Dxs representing the offset from the meteoric water line, provides information about the source conditions of water vapour. It is controlled by kinetic effects during evaporation, where a larger Dxs value is an indicator of enhanced moisture recycling and a lower value indicates an enhanced evaporative loss [40,41]. Figure 13b shows the relationship between Dxs and salinity of highly mineralized groundwater samples in Xishanzui. The δD value does not show a decreasing trend with the increase in TDS, indicating that evaporation has little influence, which is the same as the previous understanding based on the $\delta^{18}O$-TDS relationship. Therefore, Dxs in highly mineralized groundwater indicates the origin of paleo-meteoric water rather than residual seawater. In addition, the δD-value of the highly mineralized groundwater is lower than the modern average atmospheric precipitation, indicating that the recharge climate at that time was colder than that of nowadays, which is likely to be the recharge of groundwater at the end of the Late Pleistocene.

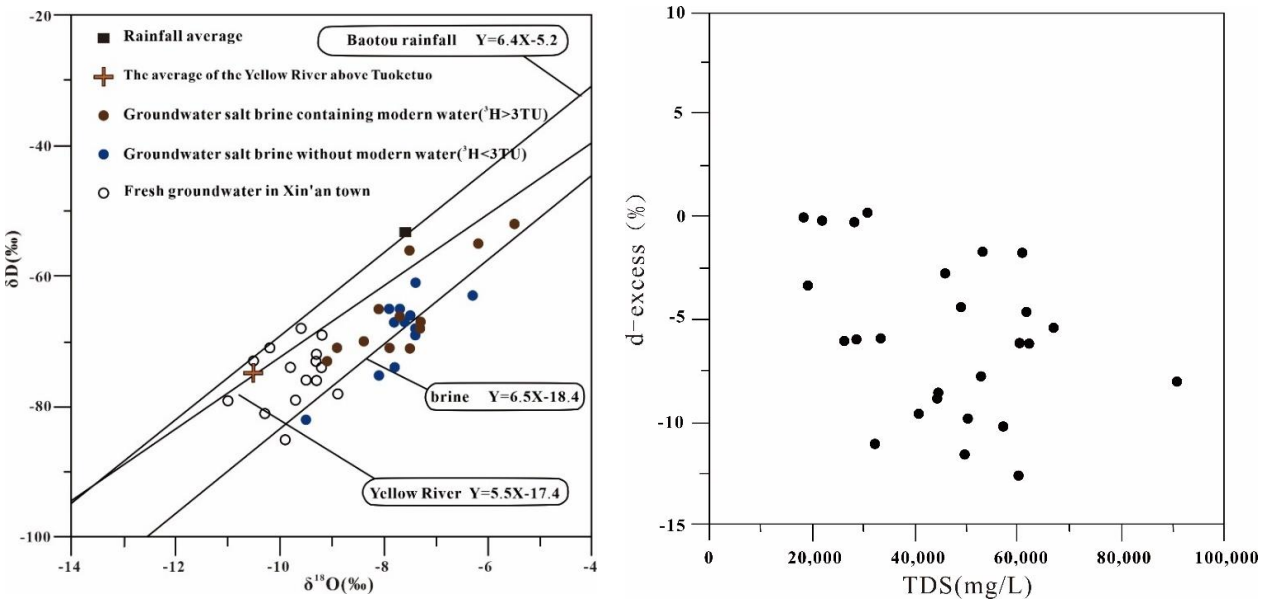

(**a**) (**b**)

Figure 13. (**a**) Hydrogen and oxygen stable isotope composition of subsurface brine in Xishanzui; (**b**) Relationship between deuterium excess and TDS of highly mineralized groundwater samples in Xishanzui.

5. Conclusions

(1) Highly mineralized water with a salinity greater than 3 g/L is widely distributed in the shallow water-bearing layer of Hetao Plain.Its area is about 3.45×10^3 km^2, accounting for 11.5% of the area of Hetao Plain. Hetao Plain can be divided into five highly mineralized water distribution zones from west to east and from north to south, namely, highly mineralized water distribution zone in front of fan depression in Houtao Plain, highly mineralized water distribution zone on the north bank of Yellow River in Houtao Plain, highly mineralized water (brine) distribution zone in Xishanzui in Houtao Plain, highly mineralized water distribution zone in Hasuhai in Hubao Plain and highly mineralized water distribution zone in Dalad Banner on the south bank of Yellow River;

(2) In the Hetao Plain, there are five highly mineralized water distribution zones from east to west and from north to south. Saline water with salinity less than 0.3 g/L is the main one, and brine with salinity greater than 10 g/L and up to 70 g/L is only distributed in Xishanzui of Houtao Plain. From the analysis of influencing factors and genesis of highly mineralized water, it can be seen that due to the formation of structural depression in front of fan, the long-term accumulation of water and salt in deep depression zone formed the distribution zone of highly mineralized water in northern plain; the existence of fault structure aggravates salt migration and brine infection, and makes shallow water and soil in the lower reaches of the south of Houtao Plain saline, which is the main reason for the formation of highly mineralized water in Xishanzui of Houtao Plain. Evaporation-concentration in groundwater drainage area and modern continental salinization are the main factors for the formation of other highly mineralized water distribution zones in the basin;

(3) According to the analysis of Piper, Gibbs diagrams of groundwater, the proportion coefficients of various components and the isotopic indications, it can be seen that most of the chemical ions in groundwater in the highly mineralized zone come from evaporation-concentration mainly affected by climate, sedimentary environment, hydrogeological conditions and hydrology. Groundwater in front of fan depression in Houtao plain, north bank of Yellow River and highly mineralized water area in Xishanzui highly mineralized water distribution zone may be recharged by deep

marine sedimentary groundwater. The sources of the highly mineralized water in Xishanzui of Houtao Plain are different from those of the highly mineralized water in other zones. Deuterium excess in highly mineralized groundwater indicates that it is of paleo-meteoric origin rather than residual seawater. The δ-D value of the highly mineralized groundwater is lower than the modern average atmospheric precipitation, which indicates that the recharge climate was colder than that of the present, and it is likely that the groundwater was replenished at the end of the Late Pleistocene. The water quality of highly mineralized shallow water in this area is formed by the mixture of deep confined water and shallow water, showing that the deep confined water in this zone can support and replenish the shallow water, and that the brine in Xishanzui highly mineralized water zone in Houtao Plain is influenced by deep underground brine.

Author Contributions: Methodology, Y.C.; software, W.C., D.Z. and X.S.; validation, Q.D. and Y.C.; formal analysis, Y.R.; writing—original draft preparation, Q.D., J.L. and D.W.; writing—review and editing, Y.C. and J.L.; funding acquisition, Y.C. All authors have read and agreed to the published version of the manuscript.

Funding: This research was funded by National Natural Science Foundation of China (41972262), Hebei Natural Science Foundation for Excellent Young Scholars(D2020504032).

Institutional Review Board Statement: Not applicable.

Informed Consent Statement: Not applicable.

Data Availability Statement: Not applicable.

Acknowledgments: Sincere thanks are given to the journal editors and anonymous reviewers for their valuable comments and suggested revisions.

Conflicts of Interest: The authors declare no conflict of interest.

References

1. Tong, Y.; Li, L.; Wang, X.; Li, Y. Revision of Handbook of Hydrogeology (2nd Edition). *J. Groundw. Sci. Eng.* **2013**, *1*, 41–47.
2. Kulmatov, R.A.; Adilov, S.A.; Khasanov, S. Evaluation of the spatial and temporal changes in groundwater level and mineralization in agricultural lands under climate change in the Syrdarya province, Uzbekistan. *IOP Conf. Ser. Earth Environ. Sci.* **2020**, *614*, 012149. [CrossRef]
3. Choudhury, K.; Saha, D.K.; Chakraborty, P. Geophysical study for saline water intrusion in a coastal alluvial terrain. *J. Appl. Geophys.* **2001**, *46*, 189–200. [CrossRef]
4. Zhang, W.K.; Yu, K.; Li, Y.Z.; Ji, X.Y.; Li, D.; Zhao, Z.; Jiang, X. Research progress of groundwater environment in Hetao Plain. *Environ. Chem.* **2020**, *39*, 489–499.
5. Zhang, H. The migration dynamics and the speciation of arsenic in the Hetao area, Inner Mongolia. *Environ. Monit. Assess.* **2020**, *192*, 332. [CrossRef] [PubMed]
6. Foster, S.; Chilton, J.; Nijsten, G.-J.; Richts, A. Groundwater—A global focus on the 'local resource'. *Curr. Opin. Environ. Sustain.* **2013**, *5*, 685–695. [CrossRef]
7. Fuoco, I.; De Rosa, R.; Barca, D.; Figoli, A.; Gabriele, B.; Apollaro, C. Arsenic polluted waters: Application of geochemical modelling as a tool to understand the release and fate of the pollutant in crystalline aquifers. *J. Environ. Manag.* **2022**, *301*, 113796. [CrossRef] [PubMed]
8. Chucuya, S.; Vera, A.; Pino-Vargas, E.; Steenken, A.; Mahlknecht, J.; Montalvan, I. Hydrogeochemical Characterization and Identification of Factors Influencing Groundwater Quality in Coastal Aquifers, Case: La Yarada, Tacna, Peru. *Int. J. Environ. Res. Public Health* **2022**, *19*, 2815. [CrossRef] [PubMed]
9. Cunrong, G. Research on the mechanism of arsenic pollution in groundwater in the Hetao Plain, Inner Mongolia, China. *Chin. J. Geol. Hazard. Control* **1999**, *10*, 25–32.
10. Guo, H.; Zhang, B.; Yang, S.; Li, Y.; Stueben, D.; Norra, S.; Wang, J. Role of colloidal particles for hydrogeochemistry in As-affected aquifers of the Hetao Basin, Inner Mongolia. *Appl. Geochem.* **2009**, *43*, 227–234. [CrossRef]
11. He, J.; Ma, T.; Deng, Y.; Yang, H.; Wang, Y. Environmental geochemistry of high arsenic groundwater at western Hetao plain, Inner Mongolia. *Front. Earth Sci.* **2009**, *3*, 63. [CrossRef]
12. Xu, X.; Huang, G.; Qu, Z.; Pereira, L.S. Assessing the groundwater dynamics and impacts of water saving in the Hetao Irrigation District, Yellow River basin. *Agric. Manag. Water Qual.* **2010**, *98*, 301–313.

13. Wang, H.-Y.; Guo, H.-M.; Xiu, W.; Bauer, J.; Sun, G.-X.; Tang, X.-H.; Norra, S. Indications that weathering of evaporite minerals affects groundwater salinity and As mobilization in aquifers of the northwestern Hetao Basin, China. *Appl. Geochem.* **2019**, *109*, 104416. [CrossRef]
14. Zhang, Z.; Guo, H.; Zhao, W.; Liu, S.; Cao, Y.; Jia, Y. Influences of groundwater extraction on flow dynamics and arsenic levels in the western Hetao Basin, Inner Mongolia, China. *Hydrogeol. J.* **2018**, *26*, 1499–1512. [CrossRef]
15. Yu, J.; Jiao, Y.; Yang, W.; Yang, J.; Liu, L. Hydrogeochemical characterization of a possible carbon sink from shallow saline–alkaline groundwater in the eastern Hetao Basin of Inner Mongolia in China. *Environ. Sci. Process. Impacts* **2021**, *23*, 344–356. [CrossRef] [PubMed]
16. Guo, H.; Zhang, Y.; Xing, L.; Jia, Y. Spatial variation in arsenic and fluoride concentrations of shallow groundwater from the town of Shahai in the Hetao basin, Inner Mongolia. *Appl. Geochem.* **2012**, *27*, 2187–2196. [CrossRef]
17. Payen, S.; Basset-Mens, C.; Núñez, M.; Follain, S.; Grünberger, O.; Marlet, S.; Perret, S.; Roux, P. Salinisation impacts in life cycle assessment: A review of challenges and options towards their consistent integration. *Int. J. Life Cycle Assess.* **2016**, *21*, 577–594. [CrossRef]
18. Schuler, M.S.; Cañedo, A.M.; Hintz, W.D.; Dyack, B.; Birk, S.; Relyea, R.A. Regulations are needed to protect freshwater ecosystems from salinization. *Philos. Trans. R. Soc. B* **2018**, *374*, 1764. [CrossRef] [PubMed]
19. Singh, A. Salinization and drainage problems of agricultural land. *Irrig. Drain.* **2020**, *69*, 844–853. [CrossRef]
20. Fuoco, I.; Marini, L.; De Rosa, R.; Figoli, A.; Gabriele, B.; Apollaro, C. Use of reaction path modelling to investigate the evolution of water chemistry in shallow to deep crystalline aquifers with a special focus on fluoride. *Sci. Total Environ.* **2022**, *830*, 154566. [CrossRef] [PubMed]
21. Kohfahl, C.; Rodriguez, M.; Fenk, C.; Menz, C.; Benavente, J.; Hubberten, H.; Meyer, H.; Paul, L.; Knappe, A.; López-Geta, J.A. Characterising flow regime and interrelation between surface-water and ground-water in the Fuente de Piedra salt lake basin by means of stable isotopes, hydrogeochemical and hydraulic data. *J. Hydrol.* **2008**, *351*, 170–187. [CrossRef]
22. Hidalgo, M.C.; Cruz-Sanjulián, J. Groundwater composition, hydrochemical evolution and mass transfer in a regional detrital aquifer (Baza basin, southern Spain). *Appl. Geochem.* **2001**, *16*, 745–758. [CrossRef]
23. Zhang, X.; Jiao, J.J.; Li, H.; Luo, X.; Kuang, X. Effects of Downward Intrusion of Saline Water on Nested Groundwater Flow Systems. *Water Resour. Res.* **2020**, *56*, e2020WR028377. [CrossRef]
24. Scanlon, B. Physical controls on hydrochemical variability in the inner bluegrass karst region of central kentucky. *Ground Water.* **1989**, *27*, 639–646. [CrossRef]
25. Scanlon, B.R.; Thrailkill, J. Chemical similarities among physically distinct spring types in a karst terrain. *J. Hydrol.* **1987**, *89*, 259–279. [CrossRef]
26. Collins, A.G.; Castagno, J.L.; Marcy, V. Potentiometric determination of ammonium nitrogen in oilfield brines. *Environ. Sci. Technol.* **1969**, *3*, 274–275. [CrossRef]
27. Li, P.; Tian, R.; Xue, C.; Wu, J. Progress, opportunities, and key fields for groundwater quality research under the impacts of human activities in China with a special focus on western China. *Environ. Sci. Pollut. Res.* **2017**, *24*, 13224–13234. [CrossRef]
28. Garrels, R.M.; Thompson, M.E. A chemical model for sea water at 25 degrees C and one atmosphere total pressure. *Am. J. Sci.* **1962**, *260*, 57–66. [CrossRef]
29. Nordstrom, D.K.; Ball, J.W.; Donahoe, R.J.; Whittemore, D. Groundwater chemistry and water-rock interactions at Stripa. *Geochim. Cosmochim. Acta* **1989**, *53*, 1727–1740. [CrossRef]
30. Parrone, D.; Ghergo, S.; Frollini, E.; Rossi, D.; Preziosi, E. Arsenic-fluoride co-contamination in groundwater: Background and anomalies in a volcanic-sedimentary aquifer in central Italy. *J. Geochem. Exploration* **2020**, *217*, 106590. [CrossRef]
31. Sun, H.; Huffine, M.; Husch, J.; Sinpatanasakul, L. Na/Cl molar ratio changes during a salting cycle and its application to the estimation of sodium retention in salted watersheds. *J. Contam. Hydrol.* **2012**, *136–137*, 96–105. [CrossRef] [PubMed]
32. Yang, C.L.; Xie, Z.Y.; Pei, S.Q.; Guo, J.Y.; Zhang, L.; Dong, C.Y.; Hao, A.S.; Yang, C.Y.; Liu, C.X. Chemical characteristics of middle permian formation water and hydrocarbon preservation conditions in northwest sichuan. *IOP Conf. Ser. Earth Environ. Sci.* **2020**, *600*, 012041. [CrossRef]
33. Subba, R.N.; Dinakar, A.; Sun, L. Estimation of groundwater pollution levels and specific ionic sources in the groundwater, using a comprehensive approach of geochemical ratios, pollution index of groundwater, unmix model and land use/land cover—A case study. *J. Contam. Hydrol.* **2022**, *248*, 103990. [CrossRef]
34. Li, P.; He, X.; Guo, W. Spatial groundwater quality and potential health risks due to nitrate ingestion through drinking water: A case study in yan'an city on the loess plateau of northwest china. *Hum. Ecol. Risk. Assess.* **2019**, *25*, 11–31. [CrossRef]
35. Fisher, R.S.; William, F.; Mullican, I. Hydrochemical Evolution of Sodium-Sulfate and Sodium-Chloride Groundwater Beneath the Northern Chihuahuan Desert, Trans-Pecos, Texas, USA. *Hydrogeol. J.* **1997**, *5*, 4–16. [CrossRef]
36. Das Sharma, S.; Sujatha, D. Characterization of the water chemistry, sediment (13)C and (18)O compositions of Kolleru Lake-a Ramsar wetland in Andhra Pradesh, India. *Environ. Monit. Assess.* **2016**, *188*, 409. [CrossRef]
37. Li, Y.-P.; Jiang, S.-Y. Major cation/chlorine ratio and stable chlorine isotopic compositions of sediment interstitial water in the Brazos-Trinity Basin IV from the Gulf of Mexico (IODP 308). *J. Asian Earth Sci.* **2013**, *65*, 42–50. [CrossRef]
38. Vengosh, A.; Chivas, A.R.; Starinsky, A.; Kolodny, Y.; Zhang, B.; Zhang, P. Chemical and boron isotope compositions of non-marine brines from the Qaidam Basin, Qinghai, China. *Chem. Geol.* **1995**, *120*, 135–154. [CrossRef]

39. Gao, J.F.; Ding, T.P.; Luo, X.R.; Tian, S.H.; Li, M. δD and $\delta^{18}O$ Variations of Water in the Yellow River and Its Environmental Significance. *Acta Geol. Sin.* **2011**, *85*, 596–602.
40. Clark, K.E.; Torres, M.A.; West, A.J.; Hilton, R.G.; New, M.; Horwath, A.B.; Fisher, J.B.; Rapp, J.M.; Robles Caceres, A.; Malhi, Y. The hydrological regime of a forested tropical Andean catchment. *Hydrol. Earth Syst. Sci.* **2014**, *18*, 5377–5397. [CrossRef]
41. Cui, J.; An, S.; Wang, Z.; Fang, C.; Liu, Y.; Yang, H.; Xu, Z.; Liu, S. Using deuterium excess to determine the sources of high-altitude precipitation: Implications in hydrological relations between sub-alpine forests and alpine meadows. *J. Hydrol.* **2009**, *373*, 24–33. [CrossRef]